small NANO MICRO

DNA Delivery

Parameters Affecting the Efficient Delivery of Mesoporous Silica Nanoparticle Materials and Gold Nanorods into Plant Tissues by the Biolistic Method

*Susana Martin-Ortigosa, Justin S. Valenstein, Wei Sun, Lorena Moeller, Ning Fang, Brian G. Trewyn, Victor S.-Y. Lin, and Kan Wang**

In memory of Professor Victor S.-Y. Lin, deceased May 4, 2010

Applying nanotechnology to plant science requires efficient systems for the delivery of nanoparticles (NPs) to plant cells and tissues. The presence of a cell wall in plant cells makes it challenging to extend the NP delivery methods available for animal research. In this work, research is presented which establishes an efficient NP delivery system for plant tissues using the biolistic method. It is shown that the biolistic delivery of mesoporous silica nanoparticle (MSN) materials can be improved by increasing the density of MSNs through gold plating. Additionally, a DNA-coating protocol is used based on calcium chloride and spermidine for MSN and gold nanorods to enhance the NP-mediated DNA delivery. Furthermore, the drastic improvement of NP delivery is demonstrated when the particles are combined with 0.6 μm gold particles during bombardment. The methodology described provides a system for the efficient delivery of NPs into plant cells using the biolistic method.

Dr. S. Martin-Ortigosa, Dr. L. Moeller,[++] Prof. K. Wang
Center for Plant Transformation
Plant Sciences Institute
Iowa State University
Ames, IA 50011, USA
E-mail: kanwang@iastate.edu

Dr. S. Martin-Ortigosa, Dr. L. Moeller, Prof. K. Wang
Department of Agronomy
Iowa State University
Ames, IA 50011, USA

J. S. Valenstein, Dr. W. Sun,[+] Prof. N. Fang, Prof. B. G. Trewyn, Prof. V. S.-Y. Lin
Department of Chemistry
Iowa State University
Ames, IA 50011, USA

J. S. Valenstein, Dr. W. Sun, Prof. N. Fang, Prof. B. G. Trewyn, Prof. V. S.-Y. Lin
Ames Laboratory
US Department of Energy
Ames, IA 50011, USA

[+] Current address: Department of Chemistry, University of Washington, Seattle, WA 98195, USA

[++] Current address: Monsanto Company, Agracetus Campus, Middleton, WI 53562, USA

DOI: 10.1002/smll.201101294

1. Introduction

The application of nanotechnology to biological sciences has brought a revolution in many areas because of the unique characteristics and potentials of nanoparticles (NPs). The main applications of nanobiotechnology include biological sensing, imaging, cell targeting, and drug delivery.[1,2] Nanotechnology has been expanding into animal and human biological research mainly because cells can readily uptake NPs. However, the utility of NPs in plant science remains limited due to a characteristic architectural feature of the plant cells, the cell wall, which restricts their uptake.[3] This could be the reason why the convergence between nanotechnology and plant biology has been limited to passive uptake, monitoring, and phytotoxicity of different NPs in plants[4] or the biological synthesis of NPs.[5] Even though bombardment,[6,7] injection,[8,9] and ultrasonication[10,11] methods have been used for NP delivery into plant cells, the most common methods involve passive introduction, such as leaf uptake,[9–12] protoplast or tissue incubation, and root uptake.[13–16] Because the passive uptake processes of NPs can vary depending on the size[8,9,12,17] and properties[18] of NPs and the types of plant tissues or cell structures,[19] it is challenging to control the

delivery and function of the NPs in the particular tissues or cells that are targeted.

One of the most powerful tools for plant biotechnologists is the biolistic system for plant genetic transformation. This method has been used for the delivery of DNA into nuclear or plastid genomes of multiple plant species.[20] A gene gun allows for the mechanical introduction of DNA-coated microcarriers, made of solid tungsten or gold with diameters ranging between 0.4–1.5 μm, into plant cells. The introduction of these microcarriers inside plant cells through bombardment relies on acceleration during the shot and is, therefore, dependent on their size and density. Bombardment is considered an attractive alternative to the passive NP-uptake methods and, in fact, gene guns have been used already to introduce NPs into animal[21–22] and plant[6–7] cell systems. The NPs delivered to plant cells by the biolistic method were mesoporous silica nanoparticles (MSNs) in tobacco plantlets and maize immature embryos,[7] and nanodiamonds in banana fruits.[6] In both cases, the efficiency of NP delivery was not studied or optimized.

Here, an efficient system for the delivery of NPs into plant cells is developed through the biolistic method. The purpose of this work is not to simply test the nucleic acid delivery abilities of NPs, because the current biolistic method (using either gold or tungsten microparticles) can deliver DNA and RNA molecules to plant tissues rather effectively. The interest here is in developing systems that would allow, for example, the NP-mediated delivery of other molecules (such as chemicals or proteins) that cannot be delivered by the current methods. In our previous study,[7] gold-capped MSNs were used to encapsulate β-oestradiol (a chemical inducer) in the pore matrix and were coated with DNA carrying a β-oestradiol-induced marker gene on the exterior. Both the inducer and inducible gene were delivered into plant tissues simultaneously and performed their functions.

The type of particle used in the biolistic method is one of the most important parameters that affects delivery;[23] therefore, one of the major challenges for the delivery of NPs to plant cells is their small size and low weight compared to any typical microcarriers used in plant transformation. For DNA delivery, small size and surface characteristics of NPs can also attribute to the inefficient delivery, due partially to poor binding/attachment of DNA to NPs. Most published protocols use simple NP and DNA incubation steps and, depending on the nature of the NPs, usually a surface-functionalization step is required to promote binding.[2,22] To overcome these problems, this research is focused on the improvement of the NP density, the NP–DNA coating protocols as well as parameters in the biolistic delivery system such as: 1) increasing the density by gold plating MSN surfaces; 2) using the $CaCl_2$/Spermidine DNA-coating protocol for enhanced DNA–NP attachment; 3) cobombarding NPs with 0.6 μm gold microparticles (GPs) and DNA. These improvements were tested over two distinct types of NPs used for different biological applications, MSNs, and gold nanorods (NRs), and can provide a promising way to expand the utility of nanobiotechnology to plant sciences.

2. Results & Discussion

2.1. Improvement of MSN Delivery into Plant Cells by Altering Particle Properties, DNA-Coating Procedure, and Bombardment Parameters

2.1.1. Increasing the Density of MSN by Gold Plating

First explored was the modification of particle density, because density is a major parameter that affects delivery. In this study, MSNs with 10 nm pore size (MSN-10) were used.[24] These MSNs were around 600 nm in diameter (**Figure 1**a)

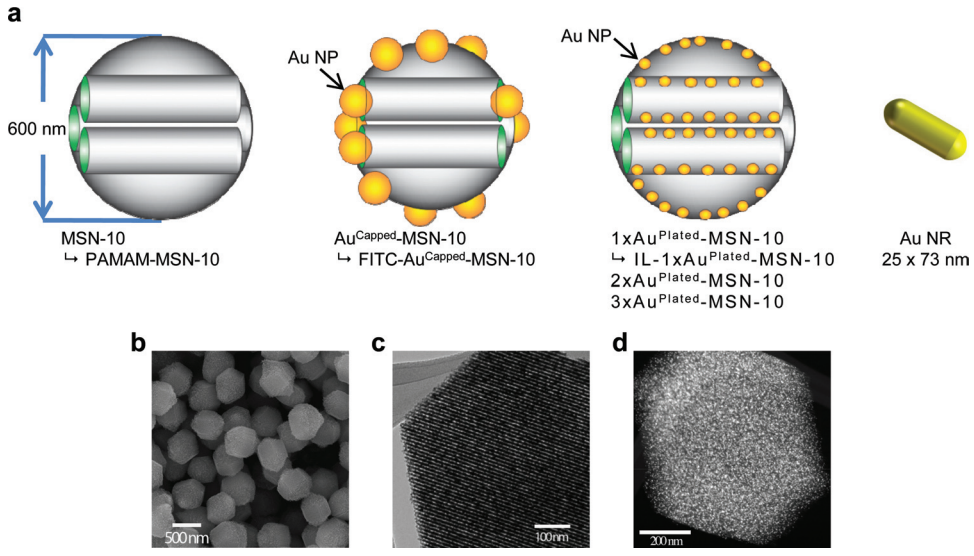

Figure 1. a) Schemes of the three different classes of MSNs and gold NRs used in this work. From left to right: MSN-10, and the PAMAM surface-functionalized MSN (PAMAM–MSN-10); gold-capped MSN-10 (Au^{Capped}–MSN-10) and the fluorescein isothiocyanate-labeled MSN (FITC–Au^{Capped}–MSN-10); 1×, 2×, or 3× gold-plated MSN-10 (1×, 2×, or 3×Au^{Plated}–MSN-10) and the ionic liquid surface-functionalized MSN (IL–1×Au^{Plated}–MSN-10); gold nanorods (Au NRs). b) SEM image of MSN-10. c) TEM image of Au^{Plated}–MSN-10. d) STEM image of Au^{Plated}–MSN-10.

NANO MICRO small

but their porous structure and the lower density of the silica material made them much lighter than a gold particle of the same size. A scanning electron microscopy (SEM) image can be seen in Figure 1b.

To increase the density of MSNs, two different strategies were designed: capping of the pores of the MSNs with gold NPs (Figure 1a, Au^{Capped}–MSN-10), or gold plating of the MSN surface. The first approach is analogous to the one described previously,[7] which was proven to allow for controlled release of the encapsulated cargo and to increase the performance of the bombardment of plant tissues.

The second approach involved plating gold on the surface of the MSNs, including the pore walls, following a similar technique reported by Zhu et al.;[25] a procedure that was repeated multiple times to increase the surface-gold loading and, thus, the density of the MSN. In this example, MSN-10 were gold-plated 1, 2, or 3 times resulting in the 1×, 2×, or 3 × Au^{Plated}–MSN-10 (Figure 1a), respectively. Transmission electron microscopy (TEM) and scanning transmission electron microscopy (STEM) images of these MSN are presented in Figure 1c,d. As is observed in Figure 1d, the gold-plating steps have produced gold nanoparticles attached to the surfaces of MSN-10, which can be seen as white dots.

The most unique feature of MSNs is their high surface area and relatively large pore size. These properties allow for the incorporation of gold via our plating method. As seen in **Table 1**, the gold plating procedures decreased both the surface area and the pore volume of the MSNs, but the final value can be considered sufficient for the encapsulation of molecules. The density of silica is 2.2 g mL^{-1} and the density of gold is 19.3 g mL^{-1}. Therefore, any amount of gold coated on the surfaces should increase the density of the MSN. Increasing the density provides the NPs more momentum during the bombardment and is expected to improve the amount of NPs introduced into plant cells. Both the gold-capping and gold-plating processes involve the use of gold to increase the density, but the gold-plating technique seems to allow more gold due to the amount of surface area capable of plating compared to the number of pores that can be capped per MSN. The gold-plating method can be considered a more straightforward technique that does not involve the synthesis of gold NPs, attachment to the pore entrances, and subsequent uncapping to release the encapsulated molecules.

2.1.2. Procedures for Coating DNA onto Nanoparticles

DNA or RNA delivery to living cells is one of the most important tools in biotechnology. When this delivery is mediated through NPs it usually relies on the ability of their surface to bind electrostatically to the negatively charged nucleic acid molecules. In our previous work, the NP-DNA coating was done by simple incubation, namely, DNA and MSNs were incubated in water for 2 h before bombarded into plant cells.[7] To improve the MSN–DNA binding capability, two surface functionalization methods were tested to provide an overall positive charge on the MSN-10, which as a consequence, will be electrostatically attracted to negatively charged DNA. PAMAM–MSN-10 (Figure 1a) was surface functionalized with a polyamidoamine dendrimer (PAMAM) layer that improved the MSN–DNA complexation and consequently DNA transfection.[26] IL–1×Au^{Plated}–MSN-10 (Figure 1a) was covalently surface-functionalized with the ionic liquid (IL), 1-propyl-3-methylimidazolium bromide, to maintain a permanent positive charge on the MSN.

The negatively charged nature of MSN-10 was reflected on its negative zeta potential (–28.0 mV), while the surface-functionalized PAMAM–MSN-10 and IL–1×Au^{Plated}–MSN-10 had +30.0 and +28.1 mV, respectively. This change in the MSN surface charge led to an improved DNA binding after a 1 h incubation period. The DNA–MSN complexation experiments (**Figure 2**a) showed how both functionalized MSNs, PAMAM–MSN-10 and IL–1×Au^{Plated}–MSN-10, had a nearly complete DNA complexation in the 1:10 (DNA:MSN) ratio, while 1×Au^{Plated}–MSN-10 did not retain any of the DNA even with a 1:50 ratio. This result suggests that both

Table 1. Pore volume and surface area of MSN-10 subjected to 1×, 2×, or 3× gold-plating procedures.

	Surface area [m^2 g^{-1}]	Pore volume [mL g^{-1}]
MSN-10	385	1.04
1×Au^{Plated}–MSN-10	351	0.98
2×Au^{Plated}–MSN-10	318	0.89
3×Au^{Plated}–MSN-10	308	0.88

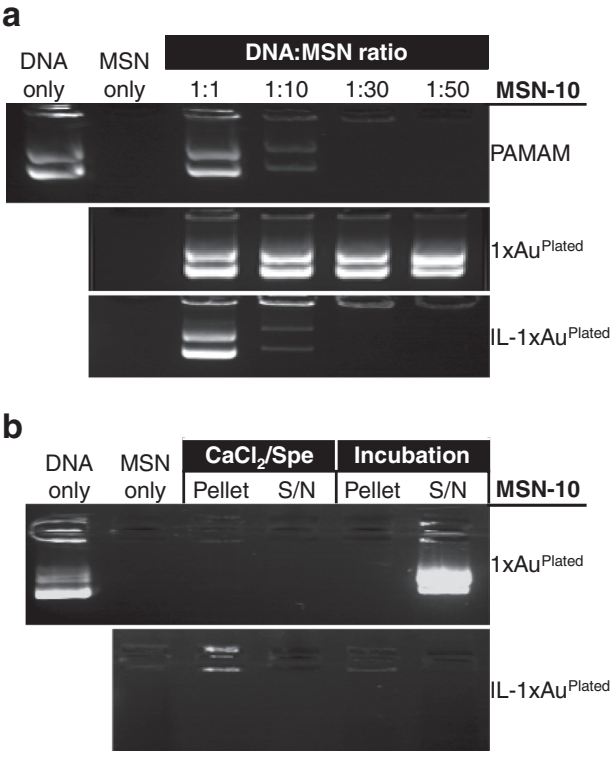

Figure 2. a) Agarose gel electrophoresis images of DNA–MSN complexation experiments of PAMAM–MSN-10, 1×Au^{Plated}–MSN-10 and IL–1×Au^{Plated}–MSN-10 at different ratios with 1 μg of DNA after 1 h incubation at room temperature. b) Agarose gel electrophoresis of the comparison of the $CaCl_2$/Spe and incubation DNA coating protocols done with 1 μg of plasmid DNA and 100 μg of 1×Au^{Plated}–MSN-10 or IL–1×Au^{Plated}–MSN-10. The pellet (DNA-coated MSN) or the supernatant (S/N, free DNA) were loaded for each procedure.

functionalizations have enhanced the DNA-binding capacity of the MSN-10 and 1×Au^{Plated}–MSN-10.

To quantitatively test the differences of these NPs and other parameters in plant cells through biolistic transformation, the number of fluorescent cells in onion epidermis tissues were measured one day after they were bombarded with MSNs coated with green fluorescent protein (GFP)- or red fluorescent protein (mCherry)-expressing plasmid DNA. The tissue can be cut into flat rectangles containing homogeneously shaped cells that facilitate the comparison between replicates and offered excellent fluorescent imaging properties.

As seen in **Figure 3**a (white bars, Incubation), under the same gene-gun conditions, more cells were transiently expressing mCherry after bombardment with the surface-functionalized IL–1×Au^{Plated}–MSN-10 (10.66 ± 5.66) than with the nonfunctionalized 1×Au^{Plated}–MSN-10 (0.33 ± 0.33). This result demonstrates that the positively charged MSN provides an advantage for DNA expression in living cells over the nonfunctionalized one, likely due to more DNA-coated MSNs being delivered into plant cells.

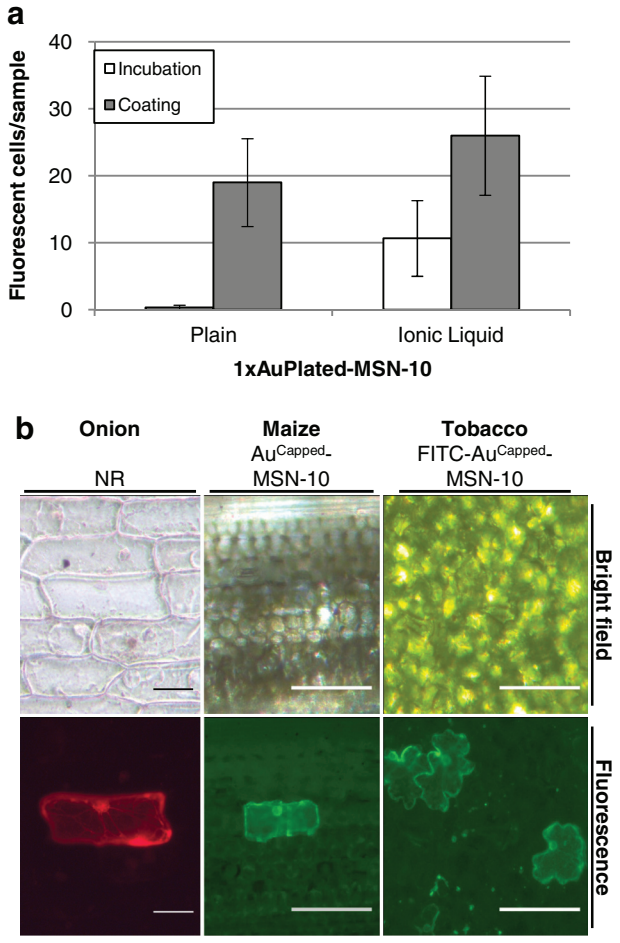

Figure 3. a) Differences on transient marker gene expression between the DNA–MSN incubation (Incubation) and $CaCl_2$/Spe DNA coating protocol (Coating) procedures onto 1×Au^{Plated}–MSN-10 (Plain) and IL–1 × Au^{Plated}–MSN-10 (Ionic Liquid). Number of red fluorescent cells per sample (2 cm × 3.5 cm onion epidermal tissue) was scored one day after bombardment using a 10× objective of Zeiss Axiostar plus microscope. b) Bright-field and fluorescence images taken with a 10× objective of Zeiss Axiostar plus microscope of plant tissues 1 day after bombardment with different types of NPs coated with GFP or mCherry expressing plasmid DNA using the $CaCl_2$/Spe coating protocol. From left to right: mCherry-expressing onion epidermis cell after bombardment with gold nanorods; GFP-expressing maize leaf cell after bombardment with Au^{Capped}–MSN-10; Tobacco leaf cells expressing GFP after bombardment with FITC–Au^{Capped}–MSN-10. Bar = 100 µm.

In a typical biolistic-mediated plant transformation procedure, DNA molecules are coated onto gold or tungsten microparticles by $CaCl_2$ and spermidine ($CaCl_2$/Spe) prior to bombardment.[27,28] The DNA–MSN incubation method was compared with the $CaCl_2$/Spe DNA-coating protocol[29] using 1×Au^{Plated}–MSN-10 (negatively charged surface) and IL–1×Au^{Plated}–MSN-10 (positively charged surface). In the MSN–DNA complexation experiments (Figure 2b), the amount of DNA and MSN used per shot in a bombardment procedure was tested for both coating protocols. The incubation protocol worked only with the positively charged surface IL–1×Au^{Plated}–MSN-10, while for the negatively charged 1×Au^{Plated}–MSN-10 all the DNA was found free in the supernatant. The $CaCl_2$/Spe protocol, on the other hand, permitted DNA complexation in both types of MSN, regardless of the charge of their surface (Figure 2b). This ability was tested on bombarded onion epidermis cells. For the same gene-gun conditions, the $CaCl_2$/Spe DNA-coating protocol worked significantly better ($P = 0.0182$) than the incubation (Figure 3a). Using the $CaCl_2$/Spe coating protocol DNA could be coated onto various NPs and to bombard different plant tissues. Figure 3b shows the delivery of either GFP- or mCherry-expressing plasmids coated onto various types of NPs such as NRs, Au^{Capped}–MSN-10 and fluorescein isothiocyanate (FITC)–Au^{Capped}–MSN-10 (Figure 1a), into onion epidermis, maize, and tobacco leaves. Two different plasmids could be coated simultaneously onto the NPs, which resulted in the coexpression of both GFP and mCherry in the same cells (data not shown).

The delivery of DNA or RNA molecules by NPs into plant cells has been reported. In all cases, the DNA–NP coating was done after 20 min to 12 h incubation.[7,11,13–15] In some cases, adding an L-lysine solution,[11] an ultrasonication step,[13] or an amino functionalization to the NP[15] had to be done to promote a DNA–NP complexation. It has been shown that this $CaCl_2$/Spe DNA-coating protocol is efficient in different types of NPs, regardless of their ionic nature. Therefore, this coating protocol is used in the rest of the experiments reported here unless otherwise indicated. This procedure may help to reduce the reliance of surface functionalization of NPs in DNA delivery, thus making it easier for the design and manufacture of the NPs.

2.1.3. Parameters Affecting Nanoparticle Delivery to Plant Cells Through Biolistics

To improve the NP delivery efficiency in plant tissues or cells, a number of parameters used in the biolistic system were tested, including target distances and the type of rupture disk. In our previous work, 650 psi rupture disks and 10 cm target distances for tobacco leaves and maize immature embryos were used.[7] Bombardment of onion epidermis tissue with Au^{Capped}–MSN-10 showed that the rupture disks for higher

NANO MICRO small

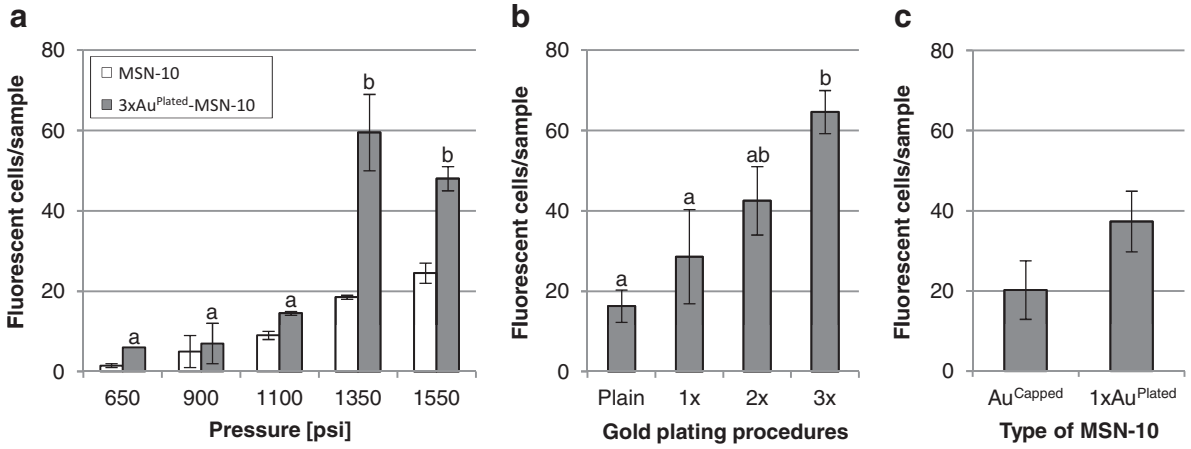

Figure 4. a) Effects of rupture disk types on MSN-10 and 3×Au^{Plated}–MSN-10 delivery efficiency. b) Effects of gold plating rounds (MSN-10, 1×, 2×, and 3×Au^{Plated}–MSN-10) on delivery efficiency. c) Comparison of the bombardment performance of Au^{Capped}–MSN-10 and 1×Au^{Plated}–MSN-10. mCherry-expressing plasmid was used in all experiments. Number of red fluorescent cells per sample (2 cm × 3.5 cm onion epidermal tissue) was scored one day after bombardment using a 10× objective of Zeiss Axiostar plus microscope. Bars in the graphs labeled with different letters indicate significantly different means according to Duncan's New Multiple Range Test ($\alpha = 0.05$).

pressures (1350 or 1550 psi) and smaller target distances (4 cm) resulted in an improved transient expression (data not shown). It was also confirmed that twice-bombarded samples had more cells transiently expressing the fluorescent proteins than the cells bombarded only once, which is in agreement with an earlier publication.[30] Therefore, all DNA–NP delivery data presented in this report utilized the twice-bombardment protocol for each sample, unless otherwise indicated.

Figure 4a shows the data comparing MSN-10 and the gold-plated 3×Au^{Plated}-MSN-10 (Figure 1a), using 5 different rupture disks. As can be seen, the number of fluorescent plant cells bombarded with MSN-10 and 3×Au^{Plated}-MSN-10 did not differ much when using rupture disk types 650, 900 and 1100 psi, respectively. However, the number of fluorescent cells after bombardment with 3×Au^{Plated}-MSN-10 increased significantly when using rupture disk types 1350 and 1550 psi ($P = 0.0017$). These data demonstrated that the increase in the density acquired during the gold plating of 3×Au^{Plated}-MSN-10 improved its performance comparing to the MSN-10 when higher pressures are used.

The delivery of four different types of gold-plated MSN-10 (MSN-10, 1×, 2×, and 3×Au^{Plated}–MSN-10) in bombarded onion epidermis cells were also compared under the same gene-gun conditions (1350 psi rupture disk and 4 cm target distance). As shown in Figure 4b, each time MSN-10 went through a gold-plating process, the increase in density enhanced its delivery to plant cells, which can be indirectly measured by the increasing number of cells expressing mCherry. The optimal MSN for DNA delivery was 3× Au^{Plated}–MSN-10, as was determined by the significantly greater number of fluorescent cells ($P = 0.015$) than MSN-10 or 1× or 2×Au^{Plated}–MSN-10 (Figure 4b).

This is the first time, to the best of our knowledge, that the gold-plating technique has been used to treat the MSN for enhancing the performance of delivery to plant cells by the biolistic method. The 1×Au^{Plated}–MSN-10 also showed better performance than the Au^{Capped}–MSN-10 (Figure 4c). Compared to the Au^{Capped}–MSN, the Au^{Plated}–MSN is easier to manufacture and allows for more functionalization. For example, caps for the Au^{Capped}–MSN are limited to just gold nanoparticles, while any 'hard' or 'soft' cap available can be utilized with the Au^{Plated}–MSN.[31] This allows us more freedom to design a delivery system tailored around the cell type and cargo of interest. While each gold-plating process increases the density of MSN, it also decreases surface area and pore volume proportionally (Table 1). Therefore, a balance between those factors needs to be determined and tested for each case.

2.2. Co-bombardment of Nanoparticles with Solid 0.6 μm Gold Microparticles for Efficient Delivery Through the Biolistic Method

In an attempt to extend the biolistic delivery system for plant cells to different types of NPs, the possibility of utilizing the commercially available 0.6 μm gold particles (GPs)—a standard microcarrier for delivering DNA in biolistic-mediated plant transformations—was explored as a microcarrier for various NPs. It was hypothesized that the NPs would attach to the GPs in the presence of DNA molecules and/or chemicals such as $CaCl_2$ and spermidine. This type of NP–GP–DNA complex would more readily penetrate plant tissues through bombardment.

Using two types of NPs different in size and nature, Au^{Capped}–MSN-10 or gold NRs (Figure 1a), four different treatments involving different NP, GP, and DNA combinations and delivery strategies were tested. **Figure 5**a summarizes the four treatments and their results. In Treatment #1 (Figure 5a, S1:cNP/S2:cNP), plant samples were bombarded twice with either DNA-coated NRs (mCherry NR) or MSNs (mCherry MSN). This treatment yielded 4 ± 3 (NR) or 12 ± 11 (MSN) fluorescent cells per sample on average as was

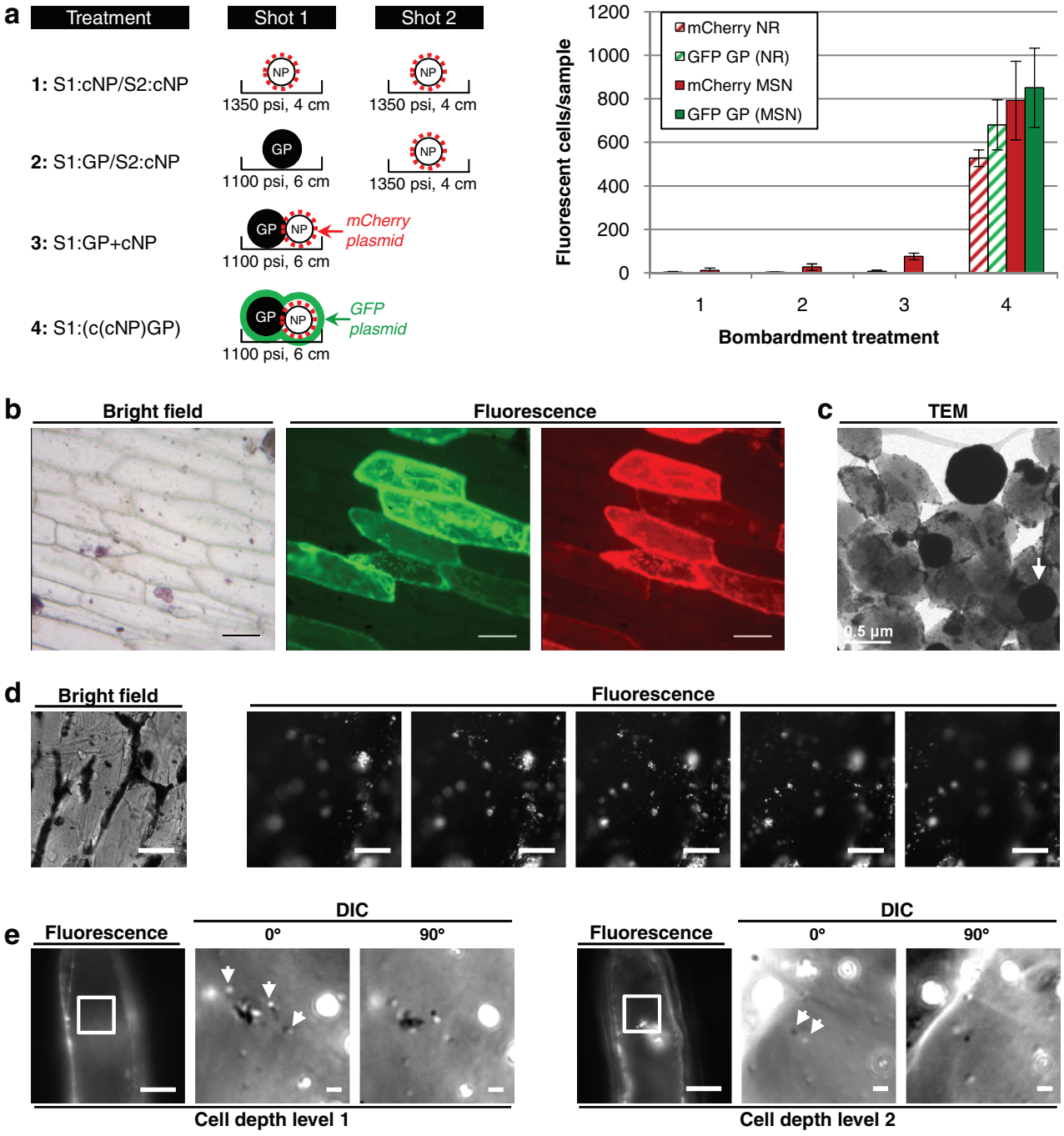

Figure 5. a) Schemes showing NP (Au^{Capped}–MSN-10 or gold NR)–GP co-bombardment treatments (left) and a graph showing the effects in NPs delivery to onion epidermis cells (right). S1: shot 1; S2: shot 2; NP: nanoparticle; GP: 0.6 µm gold; cNP, cNR and cMSN: DNA coated NP, NR or MSN respectively. Treatment #1 (S1:cNP/S2:cNP): two shots with mCherry-expressing, plasmid-coated NPs. Treatment #2 (S1:GP/S2:cNP): first shot with uncoated 0.6 µm gold and second shot with coated NPs. Treatment #3 (S1:GP+cNP): the macrocarrier was loaded first with an aliquot of uncoated 0.6 µm gold and after the DNA-coated NPs. One shot of this mixture was bombarded to plant tissues. Treatment #4 (S1:(c(cNP)GP)): one shot with a double DNA-coating procedure, first mCherry-expressing plasmid is coated onto NPs and then a second coating procedure is performed on the mixture of these particles, with 0.6 µm gold and GFP-expressing plasmid. In Treatments #2 and #3 where uncoated 0.6 µm gold was used, 2 µL aliquot of 0.6 µm gold (from a 30 µg μL^{-1} in sterile ddH_2O stock) was centrifuged at 5000 rpm, removed the supernatant, resuspended in 5 µL of ethanol and loaded in the macrocarrier. b) Bright-field and fluorescence images of onion epidermis cells expressing GFP and mCherry after co-bombardment with the Au^{Capped}–MSN-10 and 0.6 µm gold complex c(c(Au^{Capped}–MSN-10)GP). Bar = 100 µm. c) TEM image of the (c(cAu^{Capped}–MSN-10)GP) complex. d) Onion epidermis tissue bombarded with S1:c(FITC–Au^{Capped}–MSN-10+GP) complex. Bright-field image on the left and then subsequent fluorescence images of a *Z*-stack of the tissue in which focused MSNs can be seen along the depth of the cell. Bar = 10 µm, distance between *Z*-stack images = 1.5 µm. e) Two layers at different depths of an mCherry-expressing onion epidermis cell after bombardment with S1:c(NR+GP) complex. For each layer the fluorescence image (left) and an amplified image corresponding to the white square of the 2 consecutive and rotated (0 and 90°) DIC images are shown. In these images, several nanorods (white arrows) can be detected by the change in light emission on the rotated images. Bar in fluorescence images = 50 µm; in DIC images = 1 µm.

NANO MICRO small

typically observed in our study. In Treatment #2 (Figure 5a, S1:GP/S2:cNP), the samples were first bombarded with the GP followed by a second shot with the DNA-coated NPs. This was to test whether the holes on the cell walls made by the GPs would ease the following NP introduction. However, this treatment did not enhance the delivery of NP–DNA into plant cells as indicated by the number of fluorescent cells (4 ± 1 and 27 ± 15 for NR and MSN, respectively).

In Treatment #3 (Figure 5a, S1:GP+cNP), GP was first loaded onto the macrocarrier followed by the loading of DNA-coated NPs, and plant tissues were bombarded once. In this treatment, a slight increase of red fluorescent cells (76 ± 15) can be observed in samples bombarded with GP+MSN complex (mCherry MSN). The results of Treatments #2 and #3 suggest that the delivery of MSNs, not NRs, could be enhanced by the mixture of DNA-coated NPs and GPs on the macrocarrier.

In Treatment #4 (Figure 5a, S1:c(cNP)GP)), first the mCherry-expressing plasmid DNA was coated onto the NPs and then, the coated NPs were washed three times with ethanol to get rid of any free DNA molecules. The GP and a GFP-expressing plasmid DNA were then added for a second round of the $CaCl_2$/Spe coating procedure. Plant tissues were bombarded once using this c(cNP)GP complex. As can be seen in the graph of Figure 5a, this treatment led to a drastic improvement of NP delivery, indirectly indicated by the expression of both mCherry for NP delivery (mCherry NR or MSN) and GFP for GP delivery (GFP GP (NR) or (MSN)). This treatment resulted in around 130 times better for NR delivery and over 60 times in the case of MSN. Both red and green fluorescent proteins were expressed in 77% (NR) or 93% (MSN) of the cells, indicating the co-delivery of both GPs and NPs (Figure 5b). In both MSN and NR delivery experiments, the number of green fluorescent cells was slightly higher than the number of red fluorescent cells. This may suggest that more GPs than NPs were delivered by this procedure. It was also confirmed that a single DNA-coating procedure for a mixture of GP and NP, c(GP+NP), was also effective for co-bombardment (data not shown).

The c(GP+MSN) complex was examined under TEM. Figure 5c shows an example of a heterogeneous population of MSNs and GPs (white arrows). While this delivery strategy has been efficient and reproducible in our hands with onion epidermal tissues, this type of particle agglomeration can cause excessive damage to plant tissues upon bombardment. Therefore, an adequate ratio of NPs and GP and biolistic gun parameters needs to be tested for different types of plant tissues.

Further evidence for the presence of NPs inside plant cells using GPs as a carrier was collected by performing optical sectioning of the sample with either fluorescence microscopy or differential interference contrast (DIC) microscopy with the aid of a high-precision, motorized rotary stage. As shown in Figure 5d, after the c(GP+FITC–Au^{Capped}–MSN-10) complex bombardment, the FITC-labeled MSNs were found to be distributed in different axial planes of the bombarded onion epidermis cells, confirming the introduction of multiple MSNs inside the tissue. For NR detection we examined, after bombardment with the c(GP+NR) complex, mCherry-expressing onion cells. Multiple NRs (white arrows in Figure 5e) could be identified based on the change of the DIC image patterns at 0° and 90°: after rotating 90°, the DIC images of NRs changed from dark to bright or from bright to dark; while the DIC images of other cellular organelles did not have such an effect.[32] In addition, NRs were detected inside a red fluorescent cell at two planes located at different depths which confirms that this method can deliver multiple NRs and DNA into the same cell. This strategy also worked in different NP delivery in other plant explants like tobacco or maize leaf tissues (data not shown).

Using this co-bombardment strategy, we were able to effectively introduce two different types of NPs, MSNs, and NRs, into plant cells. This suggests that the strategy may be applicable to NPs of different sizes, shapes, and properties. In mammalian cell systems, the use of a complex formed by the mixture of DNA, NPs, and microparticles has been reported.[33] In this case, a complex of plasmid DNA, surface-functionalized 36 nm gold NPs and 1.5 μm gold microparticles was formed by electrostatic attachment. The goal was to deliver large amounts of DNA to mouse NIH 3T3 fibroblast cells and ear tissue by biolistics. In our case, the particles were not subjected to any surface functionalization, smaller (0.6 μm) microparticles were used, and only 1 μg of DNA was coated using the $CaCl_2$/Spe protocol.

3. Conclusion

In this study, three methods were demonstrated to improve the introduction of nanoparticles and DNA into plant cells through the biolistic system. For the first time, gold plating of MSNs was described as a way to increase the density and performance in biolistic-mediated delivery. This improvement allows the introduction of MSNs into plant cells more efficiently. Even though this gold-plating technique can diminish the porosity of MSN and, as a result, the cargo capacity, it still helps to overcome the disadvantages of bombarding plant tissues with MSNs or other types of NP, when applicable, due to their smaller size and density.

Secondly, it was shown that the $CaCl_2$/Spe DNA-coating protocol, routinely used in gold or tungsten microparticles in plant transformation, is suitable for the NPs used in this study. Using the $CaCl_2$/Spe coating method, instead of DNA–NP incubation protocol, NP-mediated DNA delivery efficiency can be improved. This coating method is applicable to different kinds of NPs (NRs and MSNs) regardless of their surface ionic state. Therefore, this method could reduce the burden of surface-functionalization steps designed to improve DNA binding capacity.

Finally, we have shown that the complex formed by NPs, GPs, and DNA after performing the $CaCl_2$/Spe coating protocol significantly enhances the introduction of NPs to plant cells through bombardment. For each particular case, the NP/GP ratio should be tested to balance the possible mechanical damage to plant cells upon bombardment.

Our group has previously reported the biolistic delivery of Au^{Capped}–MSN with 3 nm pore size into plant cells.[7] While the delivery was successful, the procedures and various

parameters in the early work were not optimized. We believe that the methodology presented in this work will provide an improved efficient method to the plant research community, representing a step forward in the transfer of advantages and applications of nanobiotechnology to plant science.

4. Experimental Section

Mesoporous Silica Nanoparticle (MSN) Synthesis: All the MSN-10 used were synthesized as described previously.[24] Briefly, the nonionic surfactant Pluronic P104 (7.0 g) was added to 1.6 M HCl (273.0 g). After stirring for 1 h at 55 °C, tetramethylorthosilicate (TMOS, 10.64 g) was added and stirred for an additional 24 h. The resulting mixture was further hydrothermally treated for 24 h at 150 °C in a high-pressure reactor. Upon cooling to room temperature (RT), the white solid was collected by filtration, washed with copious amounts of methanol, and dried in air. To remove the surfactant P104, the silica material was heated to 550 °C at a ramp rate of 1.5 °C min^{-1} and maintained at 550 °C for 6 h. The fluorescein isothiocyanate (FITC) labeling of Au^{Capped}–MSN-10 was done by adding 5 mg (12.8 μmol) of FITC to 3-aminopropyltrimethoxysilane (APTMS, 13 μmol) in dry DMSO (0.5 mL) and stirred for 30 min, and then added to a toluene suspension (100 mL) of MSN-10 (1.0 g). The suspension was refluxed for 20 h under nitrogen and the resulting material was filtered, washed with toluene and methanol, and dried under vacuum overnight.

For Au^{Capped}–MSN-10, 3-mercaptopropyltrimethoxysilane (MPTMS, 2 mmol) was grafted to MSN-10 (1.0 g) by refluxing in toluene (100 mL) for 20 h under nitrogen. The resulting thiol-functionalized MSN (thiol–MSN-10) was filtered, washed with toluene and methanol, and dried under vacuum overnight. To activate thiol–MSN-10, 2,2-dipyridyldisulfide (3 mmol) was added to a methanol suspension of the thiol–MSN-10 and stirred for 24 h in the absence of light. The resulting material was filtered, washed with methanol, and dried under vacuum overnight. To synthesize amine-linker–MSN-10 (2-(propyldisulfanyl)ethylamine–MSN-10), 2-aminoethanethiol (3 mmol) was added to a methanol suspension of the activated thiol–MSN-10 and stirred for 24 h. The resulting material was filtered and washed with methanol, and dried under vacuum overnight. Carboxylic acid-functionalized gold NPs (25 mg, AuNP–COOH) were suspended in phosphate-buffered saline (PBS) solution (3 mL) along with *N*-ethyl-*N'*-(3-dimethylaminopropyl)carbodiimide (EDC, 100 mg) and *N*-hydroxysuccinimide (NHS, 80 mg) and stirred for 15 min. Amine linker–MSN-10 (50 mg) was added to the mixture and stirred for 24 h. The Au^{Capped}–MSN were collected by centrifugation, washed three times with water, and then resuspended in water (5 mL), frozen in liquid nitrogen, and dehydrated in a lyophilizer.

For PAMAM–MSN-10 synthesis, MPTMS (2 mmol) was added to a toluene suspension (100 mL) of MSN-10 (1.0 g) and refluxed for 20 h under nitrogen, then filtered, washed with toluene and methanol, and dried under vacuum overnight. The thiol–MSN-10 was activated by the same method as previously described for the amine-linker–MSN-10, instead of 2-aminoethanethiol, an equimolar amount of 11-mercaptoundecanoic acid was added to a methanol suspension (acid-linker–MSN-10). Acid-linker–MSN-10 (20 mg) was suspended in PBS solution (3 mL) and EDC (100 mg), and NHS (80 mg) was added and stirred for 15 min. PAMAM–G4 dendrimer (25 mg) was added to the mixture, stirred for 24 h. The particles were collected by centrifugation, washed three times with water, resuspended in water (5 mL), frozen in liquid nitrogen, and dehydrated in a lyophilizer.

For the gold $1\times Au^{Plated}$–MSN-10, ethylenediamine (0.45 mL) was added to an aqueous solution of $HAuCl_4 \cdot 3H_2O$ (1.0 g) in water (10 mL), stirred for 30 min and followed by the addition of ethanol (70 mL). The resulting $Au(en)_2Cl_3$ precipitate was filtered, washed with ethanol, dried under vacuum and, after that, 0.372 g was dissolved in H_2O (150 mL) and the pH adjusted to 10.0 using NaOH. MSN-10 (2 g) was added to the solution, the pH was readjusted to 9.0 with NaOH, and this was stirred for 2 h. The product was filtered and dried under vacuum for 2 days, and then reduced under H_2 flow at 150 °C for 3 h. For the ionic liquid layer functionalization of IL–$1\times Au^{Plated}$–MSN-10, 1-propyltriethoxysilane-3-methylimidazolium chloride (PMIm, 2 mmol) was added to an *N*,*N*-dimethylformamide suspension (DMF, 100 mL) of Au–MSN-10 (1.0 g) and then refluxed for 20 h under nitrogen. The resulting material was filtered, washed with DMF and methanol, and dried under vacuum overnight. To synthesize 2× and $3\times Au^{Plated}$–MSN-10, $1\times Au^{Plated}$–MSN-10 was subjected to the $Au(en)_2$ impregnation and reduction process an additional one and two more cycles, respectively.

Zeta Potential Measurements: Each sample (5 mg) was sonicated in PBS (10 mL) for 30 min. The samples were then analyzed on a Malvern Instruments Zetasizer.

MSN Surface Area and Porosity Measurements: The surface area and average pore diameter were measured using N_2 adsorption/desorption measurements in a Micromeritics ASAP 2020 BET surface analyzer system. The data were evaluated using BET and BJH methods to calculate surface area and pore distributions, respectively. Samples were prepared by degassing at 100 °C overnight before analysis.

Nanorods: Gold nanorods (25 nm × 73 nm, catalog number 30-25-700-100) were purchased from Nanopartz.

Plant Materials: Onion epidermis tissue was obtained from white bulk onion bulbs. The tissue was cut in 2 cm × 3.5 cm rectangles and placed with the peeled face upwards in agar media (0.5 mM 2-(*N*-morpholino)ethanesulfonic acid (MES) pH 5.7, and 15 g L^{-1} of BD Bacto agar, pH 5.7) or MS media[34] (MS salts and vitamins from PhytoTechnology Laboratories, 2% sucrose, 2.5 g L^{-1} Phytagel from Sigma Aldrich, pH 5.7). Leaf pieces of 3–4 week old maize plants of the inbred A188 germinated in soil were cut into pieces approximately 3 cm long and placed on MS media with the adaxial surface up. Leaves from 6–8 week old in-vitro grown tobacco plants (*Nicotiana tabacum* var. Petite Havana) were placed on MS media with the adaxial surface up.

DNA–MSN Complexation Experiments: MSN stocks at 10 mg mL^{-1} in sterile, double-distilled water (ddH_2O) were sonicated in a water-bath sonicator (FS6 from Fisher Scientific) for 15 s. One, 10, 30, or 50 μg of MSNs were incubated with plasmid DNA (1 μg) in a final volume of 15 μL for 1 h at RT. The total mixture was loaded in a 1% agarose gel stained with ethidium bromide and electrophoresed at 100 V for 25 min. The supernatant of the $CaCl_2$/Spe DNA-coating protocol was subjected before loading to dialysis for 30 min using a MF-Membrane filter of 0.025 μm (Millipore).

Nanoparticle DNA-Coating and Sample Bombardment: The plasmids ER-rk[35] and pLMNC95[36] for mCherry and GFP expression, respectively, were obtained from the Arabidopsis Biological Resource Center (ABRC stocks CD3-959 and CD3-420 respectively,

NANO MICRO small

http://www.arabidopsis.org). The DNA-coating and NP-bombardment procedures were done according to standard protocols[27,28] with the following modifications (protocols described for one shot): 100 μg of MSNs (from a 10 μg μL^{-1} stock in sterile ddH_2O) or 150 μL of the commercial nanorod suspension (previously washed with sterile ddH_2O after centrifuging at 2000 g for 6 min and resuspended in 10 μL of sterile ddH_2O) were sonicated for 15–30 s in a water-bath sonicator. One μg of plasmid DNA (from a 250 ng μL^{-1} stock in sterile ddH_2O), 12.5 μL of a 2.5 M of $CaCl_2$ and 5 μL of a 0.1 M spermidine solution were added to NPs and mixed for 10 min at RT. The mix was centrifuged at 5000 rpm (Spectrafuge 16M from Labnet) for 15 s at RT, the supernatant was removed, and freezer-cold 100% ethanol (60 μL) was added to wash the pellet. After another centrifugation step and removal of the supernatant, the coated NPs were resuspended in cold 100% ethanol (5 μL) and loaded in the center of a macrocarrier.

Plant tissues were bombarded with DNA-coated NPs as described.[28] A Bio-Rad PDS-1000/He biolistic gun and Bio-Rad biolistic supplies were used. Five different rupture disks (650, 900, 1100, 1350, or 1550 psi) and two different target distances (6 or 4 cm) were tested. The typical bombardment parameters used in this study for NPs were 1350 psi, 4 cm target distance, and 2 shots. The 4 cm target distance was achieved by placing the sample over a Petri dish with the bottom part upwards on the 6 cm shelf of the gene gun.

For the Treatment #4, the pellet obtained after $CaCl_2$/Spe-coating of NP with mCherry-expressing plasmid was washed and pelleted (5000 rpm, 15 s) 3 times with ethanol (60 μL) to remove any free DNA. The resulting pellet was mixed with 2 μL of 0.6 μm gold (30 μg μL^{-1} in sterile ddH_2O, Bio-Rad cat# 165-2262) and 1 μg of a 250 ng μL^{-1} stock of GFP-expressing plasmid DNA and followed by a second round of DNA coating. For the preparation of DNA-coated NP and GP mix (c(NP+GP)) the NPs were mixed by pippeting with the 2 μL of the 0.6 μm gold suspension. To this mix of particles, 1 μg of a 250 ng μL^{-1} stock of DNA plasmid was added and followed the described protocol for DNA coating. Bombardment with those two types of NP–GP mixes were made once at 1100 psi and 6 cm target distance.

Statistical Analysis: The graphs presented in Figure 3 and 4 represent the mean of 2 to 4 repeats ± standard error. The comparisons between treatments were done by ANOVA-Duncan Test (α = 0.05) using the SAS 9.2 statistical program.

Fluorescence Microscopy: Fluorescence and bright-field images were taken with a 10×A-Plan (numerical aperture, N.A. 0.25) objective of a Zeiss Axiostar plus microscope. For GFP images, an Endow GFP BP filter was used (λ_{ex} = 470 nm, beam splitter at 495 nm and λ_{em} = 525 nm); for mCherry images, a Texas Red filter was used (λ_{ex} = 560 nm, beam splitter at 595 nm and λ_{em} = 645 nm), both from Chroma Technology Corp. Images were taken with a ProgRes C3 digital camera and the ProgRes Capture Pro 2.6 software from Jenoptik, and were edited for publication using Adobe Photoshop software from Adobe Systems Inc.

Differential Interference Contrast (DIC) Microscopy: DIC and epi-fluorescence images were taken with an upright Nikon Eclipse 80i microscope. A motorized rotary stage (SGSP-60YAM, Sigma Koki) was coupled to the fine-adjustment knob on the microscope to help image sample areas with different depths. For the DIC mode, the samples were illuminated through an oil immersion condenser (N.A. 1.40) and the optical signals were collected with a 100×Plan Apo N.A.1.40 oil immersion objective. One bandpass filter with central wavelength in 700 nm and a full width at half maximum of 13 nm was inserted into the light path in the microscope. For the fluorescence images, a filter cube containing one 480 nm bandpass filter, one 500 nm dichroic mirror and one 530 nm bandpass filter was used. The optical filters were obtained from Semrock. An Andor iXon^{EM}+ camera (512 × 512 imaging array, 16 μm × 16 μm pixel size) and the software ImageJ were used to record and analyze the DIC and fluorescence images.

TEM, SEM, and STEM Imaging: TEM and STEM investigations were done by placing small aliquot of an aqueous suspension on a lacey carbon film coated 400 mesh copper grid and drying it in air. The TEM images were obtained on a Tecnai F^2 microscope. Particle morphology was determined by SEM using a Hitachi S4700 FE-SEM system with 10 kV accelerating voltage.

Acknowledgements

SMO and KW thank Angela Nguyen for technical support and Xing Xu for statistical analysis support. This work is partially supported by Plant Sciences Institute of Iowa State University and Pioneer Hi-Bred International, Inc.

[1] a) N. O'Farrell, A. Houlton, B. R. Horrocks, *Int. J. Nanomedicine* **2006**, *1*, 451; b) J. Stone, S. Jackson, D. Wright, *Wiley Interdisciplinary Reviews: Nanomedicine and Nanobiotechnology* **2011**, *3*, 100; c) O. V. Salata, *J. Nanobiotechnol.* **2004**, *2*, 3.

[2] I. I. Slowing, J. L. Vivero-Escoto, B. G. Trewyn, V. S.-Y. Lin, *J. Mater. Chem.* **2010**, *20*, 7924.

[3] C. M. Rico, S. Majumdar, M. Duarte-Gardea, J. R. Peralta-Videa, J. L. Gardea-Torresdey, *J. Agric. Food Chem.* **2011**, *59*, 3485.

[4] a) R. Nair, S. H. Varghese, B. G. Nair, T. Maekawa, Y. Yoshida, D. S. Kumar, *Plant Sci.* **2010**, *179*, 154; b) X. Ma, J. Geiser-Lee, Y. Deng, A. Kolmakov, *Sci. Total Environ.* **2010**, *408*, 3053.

[5] K. N. Thakkar, S. S. Mhatre, R. Y. Parikh, *Nanomed. Nanotechnol. Biol. Med.* **2010**, *6*, 257.

[6] V. Grichko, V. Grishko, O. Shenderova, *NanoBioTechnol.* **2006**, *2*, 37.

[7] F. Torney, B. G. Trewyn, V. S.-Y. Lin, K. Wang, *Nat. Nanotechnol.* **2007**, *2*, 295.

[8] P. González-Melendi, R. Fernández-Pacheco, M. J. Coronado, E. Corredor, P. S. Testillano, M. C. Risueño, C. Marquina, M. R. Ibarra, D. Rubiales, A. Pérez-de-Luque, *Ann. Bot.* **2008**, *101*, 187.

[9] E. Corredor, P. Testillano, M.-J. Coronado, P. González-Melendi, R. Fernández-Pacheco, C. Marquina, M. R. Ibarra, J. de la Fuente, D. Rubiales, A. Perez-de-Luque, M. C. Risueño, *BMC Plant Biol.* **2009**, *9*, 45.

[10] Q. Wang, J. Chen, H. Zhang, M. Lu, D. Qiu, Y. Wen, Q. Kong, *J. Nanosci. Nanotechnol.* **2011**, *11*, 2208.

[11] J. Liu, F.-H. Wang, L.-L. Wang, S.-Y. Xiao, C.-Y. Tong, D.-Y. Tang, X.-M. Liu, *J. Cent. S. Univ. Technol.* **2008**, *15*, 768.

[12] a) K. Birbaum, R. Brogioli, M. Schellenberg, E. Martinoia, W. J. Stark, D. Günther, L. K. Limbach, *Environ. Sci. Technol.* **2010**, *44*, 8718; b) T. Eichert, A. Kurtz, U. Steiner, H. E. Goldbach, *Physiol. Plant* **2008**, *134*, 151.

[13] Q. Liu, B. Chen, Q. Wang, X. Shi, Z. Xiao, J. Lin, X. Fang, *Nano Lett.* **2009**, *9*, 1007.

[14] a) K. Pasupathy, S. Lin, Q. Hu, H. Luo, P. C. Ke, *Biotechnol. J.* **2008**, *3*, 1078; b) A. Silva, A. Nguyen, C. Ye, J. Verchot, J. Moon, *BMC Plant Biol.* **2010**, *10*, 291.
[15] S. R. Wilson, US 20110059529A1, **2011**.
[16] a) M. F. Serag, N. Kaji, C. Gaillard, Y. Okamoto, K. Terasaka, M. Jabasini, M. Tokeshi, H. Mizukami, A. Bianco, Y. Baba, *ACS Nano* **2010**, *5*, 493; b) G. Yu, J. Liang, Z. He, M. Sun, *Chem. Biol.* **2006**, *13*, 723; c) M. Lucas, B. A. Macdonald, G. L. Wagner, S. A. Joyce, K. D. Rector, *ACS Appl. Mater. Interfaces* **2010**, *2*, 2198; d) S. Ravindran, S. Kim, R. Martin, E. M. Lord, C. S. Ozkan, *Nanotechnol.* **2005**, *16*, 1; e) E. Etxeberria, P. Gonzalez, E. Baroja-Fernandez, J. P. Romero, *Plant Signal Behav.* **2006**, *1*, 196; f) E. Onelli, C. Prescianotto-Baschong, M. Caccianiga, A. Moscatelli, *J. Exp. Bot.* **2008**, *59*, 3051; g) E. Wild, K. C. Jones, *Environ. Sci. Technol.* **2009**, *43*, 5290; h) S. Lin, J. Reppert, Q. Hu, J. S. Hudson, M. L. Reid, T. A. Ratnikova, A. M. Rao, H. Luo, P. C. Ke, *Small* **2009**, *5*, 1128; i) Q. Wang, B. Chen, P. Liu, M. Zheng, Y. Wang, S. Cui, D. Sun, X. Fang, C. M. Liu, W. J. Lucas, J. Lin, *J. Biol. Chem.* **2009**, *284*, 12000; j) Z. Cifuentes, L. Custardoy, J. de la Fuente, C. Marquina, M. R. Ibarra, D. Rubiales, A. Perez-de-Luque, *J. Nanobiotechnol.* **2010**, *8*, 26; k) M. V. Khodakovskaya, K. de Silva, D. A. Nedosekin, E. Dervishi, A. S. Biris, E. V. Shashkov, E. I. Galanzha, V. P. Zharov, *Proc. Natl. Acad. Sci. USA* **2011**, *108*, 1028.
[17] A. G. Perez-Donoso, Q. Sun, M. C. Roper, L. C. Greve, B. Kirkpatrick, J. M. Labavitch, *Plant Physiol.* **2010**, *152*, 1748.
[18] R. Chen, T. A. Ratnikova, M. B. Stone, S. Lin, M. Lard, G. Huang, J. S. Hudson, P. C. Ke, *Small* **2010**, *6*, 612.
[19] H. Zhu, J. Han, J. Q. Xiao, Y. Jin, *J. Environ. Monit.* **2008**, *10*, 713.
[20] a) H. Warzecha, A. Hennig, *Genetic Modification of Plants*, Vol. *64*, Springer, Berlin/Heidelberg **2010**, p. 23; b) T. M. Klein, *Plant Transformation Technologies*, Wiley-Blackwell, Oxford, UK **2011**, p. 53.
[21] a) H. A. Clark, M. Hoyer, S. Parus, M. A. Philbert, R. Kopelman, *Microchim. Acta* **1999**, *131*, 121; b) P. W. Lee, S. F. Peng, C. J. Su, F. L. Mi, H. L. Chen, M. C. Wei, H. J. Lin, H. W. Sung, *Biomater.* **2008**, *29*, 742.
[22] S. A. Svarovsky, M. J. Gonzalez-Moa, M. D. Robida, A. Y. Borovkov, K. Sykes, *Mol. Pharm.* **2009**, *6*, 1927.
[23] M. Zhang, W. Tao, P. A. Pianetta, *Phys. Med. Biol.* **2007**, *52*, 1485.
[24] T.-W. Kim, I. I. Slowing, P.-W. Chung, V. S.-Y. Lin, *ACS Nano* **2010**, *5*, 360.
[25] H. Zhu, C. Liang, W. Yan, S. H. Overbury, S. Day, *J. Phys. Chem. B* **2006**, *110*, 10842.
[26] D. R. Radu, C. Y. Lai, K. Jeftinija, E. W. Rowe, S. Jeftinija, V. S. Y. Lin, *J. Am. Chem. Soc.* **2004**, *126*, 13216.
[27] T. M. Klein, E. D. Wolf, R. Wu, J. C. Sanford, *Nature* **1987**, *327*, 70.
[28] J. C. Sanford, F. D. Smith, J. A. Russell, *Methods Enzymol.* **1993**, *217*, 483.
[29] B. Frame, H. Zhang, S. Cocciolone, L. Sidorenko, C. Dietrich, S. Pegg, S. Zhen, P. Schnable, K. Wang, *In Vitro Cell. Dev. Biol. Plant* **2000**, *36*, 21.
[30] T. M. Klein, M. Fromm, A. Weissinger, D. Tomes, S. Schaaf, M. Sletten, J. C. Sanford, *Proc. Natl. Acad. Sci. USA* **1988**, *85*, 4305.
[31] B. G. Trewyn, I. I. Slowing, S. Giri, H.-T. Chen, V. S.-Y. Lin, *Acc. Chem. Res.* **2007**, *40*, 846.
[32] a) G. Wang, W. Sun, Y. Luo, N. Fang, *J. Am. Chem. Soc.* **2010**, *132*, 16417; b) A. S. Stender, G. Wang, W. Sun, N. Fang, *ACS Nano* **2010**, *4*, 7667.
[33] S. Svarovsky, A. Borovkov, K. Sykes, *BioTechniques* **2008**, *45*, 535.
[34] T. Murashige, F. Skoog, *Physiol. Plant.* **1962**, *15*, 473.
[35] B. K. Nelson, X. Cai, A. Nebenführ, *Plant J.* **2007**, *51*, 1126.
[36] S. Luke Mankin, W. F. Thompson, *Plant Mol. Biol. Reporter* **2001**, *19*, 13.

Received: June 28, 2011
Revised: July 11, 2011
Published online: December 16, 2011

